Diagn Interv Radiol 2014; 20:470–474

CHEST IMAGING

ORIGINAL ARTICLE

Clinical applications of the C-arm cone-beam CT-based 3D needle guidance system in performing percutaneous transthoracic needle biopsy of pulmonary lesions

De-Chao Jiao, Teng-Fei Li, Xin-Wei Han, Gang Wu, Ji Ma, Ming-Ti Fu, Qi Sun, Janina Beilner

PURPOSE
This study explored the value of flat detector C-arm CT-guidance system in performing percutaneous transthoracic needle biopsy (PTNB) for lung lesions in clinical practice.

METHODS
A total of 110 patients with solid lung lesions were enrolled to undergo PTNB procedures. The mean diameter of lesions was 4.63 cm (range, 0.6–15cm). The needle path was carefully planned and calculated on the C-arm CT system, which acquired three-dimensional CT-like cross-sectional images. The PTNB procedures were performed under needle guidance with fluoroscopic feedbacks.

RESULTS
Histopathologic tissue was successfully obtained from 108 patients with a puncture success rate of 98.2% (108/110). The diagnostic accuracy rate was found to be 96.3% (104/108). There was only one case of pneumothorax (0.9%) requiring therapy. The rates of mild pneumothorax and hemoptysis were low (12.0% and 6.5%, respectively). In addition, procedural time could be limited with this technique, which helped to reduce X-ray exposure.

CONCLUSION
Our study shows that C-arm CT-based needle guidance enables reliable and efficient needle positioning and progression by providing real-time intraoperative guidance.

From the Department of Interventional Radiology (D.C.J., T.F.L., X.W.H. ✉ *zdyfy_han@hotmail.com*, G.W., J.M., M.T.F), The First Affiliated Hospital of Zhengzhou University, Zhengzhou, Henan, People's Republic of China; the Interventional Therapy Institute of Zhengzhou University (D.C.J., T.F.L., X.W.H., G.W., J.M., M.T.F), Zhengzhou, Henan, People's Republic of China; Siemens Healthcare (Q.S., J.B.), Siemens Ltd. China, Beijing, China.

Received 25 November 2013; revision requested 11 December 2013; final version received 26 June 2014; accepted 27 June 2014.

Published online 16 October 2014.
DOI 10.5152/dir.2014.13463

Lung cancer is the commonest cause of a pulmonary mass, which can be identified through chest X-ray or computed tomography (CT) examinations (1, 2). Accurate identification of histopathological cell type is crucial to determine the right treatment method and reduce the morbidity and mortality rates. Image-guided percutaneous transthoracic needle biopsy (PTNB) is a widely accepted technique for characterization of pulmonary mass that is not reachable by broncoscopy. CT has been considered as the technique of choice for guiding PTNB procedures as it enables detailed visualization of the lesion and surrounding tissue structures. This technique offers good in-plane resolution. However, the view is limited to the plane that the needle is inserted, causing double-oblique approach with an angulated needle trajectory which is difficult to perform, time consuming (25–27 minutes), and heavily relies on the experience of the clinicians (3). The introduction of CT fluoroscopy (CTF) enables real-time visualization of the needle advancement. Thus, the challenges correlated with displacement and disappearance of small lesions from scan planes due to respiratory movement in conventional CT-guided PTNB can be overcome, leading to a reduced procedural time (12–24 minutes) (4). Nevertheless, CTF may result in higher radiation dose to clinicians (5–9). Besides, according to previous studies, lesion size is a determining factor in diagnostic accuracy of CT- or CTF-guided PTNB, which yields 75%–90% diagnostic accuracy, with correlated rates of 15%–20% for pneumothorax and 2%–3% for pneumothorax requiring drainage (10–14). In addition, due to the limited size of the gantry, CT- or CTF-guided PTNB procedures in obese patients can be technically challenging or impossible.

Nowadays, flat detector-equipped angiographic C-arm cone-beam CT (CBCT) systems can be used to acquire CT-like cross-sectional images directly within the interventional radiology suite (15–17). The CBCT systems offer real-time visualization of PTNB procedure and more flexibility in the orientation of the detector system around the patient compared to traditional CT systems. Thus, CBCT could provide image guidance for PTNB procedures, combining the advantages of CT and fluoroscopic guidance, as it is proved to be valuable for evaluating pulmonary lesions even smaller than 2 cm. This technique has been shown to yield 90%–98% diagnostic accuracy, 94%–97% sensitivity, and 75%–100% specificity. The incidence of complications was 20%–39%, the associated procedural time ranged 11.9–18.1 minutes and exposure dose ranged 170–275 mGy (3, 18–24). Along with the development of CBCT, a novel technique has recently emerged for PTNB guidance. It combines advanced virtual needle path planning based on user interactions using three-di-

mensional (3D) CBCT images with real-time fluoroscopic guidance (21, 25). This technique offers high spatial resolution of less than 1 mm, as well as contrast resolution of 10 HU, which is adequate for lung imaging, as lung inherently has a high contrast (soft tissue against air). In addition, CBCT allows good access to the patient without any patient transfer or movement, increasing the effectiveness and efficacy of clinical workflow.

The purpose of this study is to explore the value of using a CBCT-based 3D needle guidance system in performing PTNB for pulmonary lesions in the interventional radiology suite.

Methods

Patient selection

From September 2009 to May 2011, 110 consecutive patients (77 males, 33 females; mean age, 51.6±16.8 years) with a total number of 110 solid pulmonary lesions were enrolled in this study. The mean diameter of lesions was 4.63±2.97 cm.

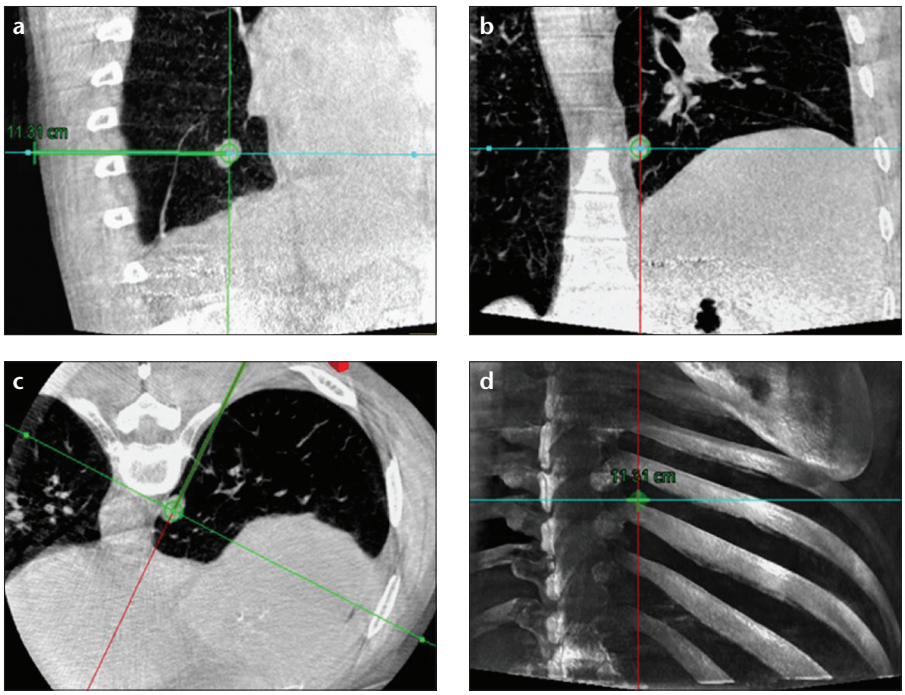

Figure 1. a–d. CBCT orthogonal multiplanar images with graphics showing planned needle path *(green line)* into target lesion *(green circle)* **(a–c)**. The cross indicates the skin entry site and the circle indicates the target lesion site. The needle position relative to the anatomical structures is displayed in 3D using volume rendering technique **(d)**.

Image acquisition

As the first step, 3D CBCT images of the patients were acquired with a rotational angiographic system (Artis zeego, Siemens Healthcare, Forchheim, Germany). During the image acquisition, the region-of-interest was positioned in the isocenter and the C-arm was rotated 200° in eight seconds. As an output, a total number of 397 projection images were generated with an X-ray dose of 0.36 µGy/frame, projection increment 0.5°, 1-k matrix, zoom factor 0, and field of view 480 mm. With the detector used, the imaged volume had a cylindrical shape of 185 mm height and 225 mm diameter, with a voxel size of 0.4 mm. The patients were asked to hold their breaths for the entire eight seconds of 3D CBCT image acquisition.

The resulting raw projection images were then automatically transferred to a post-processing workstation (*syngo* X Workplace; Siemens Healthcare) for 3D volume reconstruction. As a result, the CBCT images were reconstructed and presented in axial, sagittal, and coronal orientations. The time from the end of the image acquisition to the presentation of multiplanar images on the workstation ranged 43–45 s.

Needle path planning and guidance procedure

As the second step, the needle path was planned on the same workstation using commercially available software (*syngo* iGuide; Siemens Healthcare). Figs. 1–3 demonstrate this procedure for a 1.5 cm pulmonary lesion. The reconstructed 3D volume was loaded first. In the orthogonal multiplanar images, the skin entry point and target lesion position were manually selected and marked by a cross and a circle, respectively. A virtual path was generated with its angulations and length calculated and displayed. All three multiplanar images were automatically aligned to the defined path to provide in-plane views (Fig. 1). This procedure could be iteratively performed, modified and reviewed until a satisfying path was obtained.

In order to use the planned path to align the needle in actual 3D space, the virtual path was then projected and superimposed onto the live fluoroscopic images and displayed on a dedicated live monitor. The software automatically calculated the C-arm angulations, table motion, image zoom, and then controlled the C-arm moving to the desired position. First, the C-arm was rotated to the "bull's eye view", where it was angulated in a way that the cross and the circle displayed on live monitor completely matched and the central X-ray beam was aligned with the planned path. Thus, the skin entry point could be determined. The needle orientation was adjusted until both the tip and the hub of the needle in the fluoroscopic image were superimposed and located at the center of the circle and the cross. Second, after the skin entry point and needle orientation were determined, the needle was advanced under fluoroscopy until the planned target lesion position was reached. The C-arm was rotated back and forth to two different angles subsequently to monitor the needle progression. These two angles provided lateral views (progression view) of the planned needle path and helped to ensure that the needle was advanced along this path (Fig. 2). Third, a 3D scan was acquired to confirm the final position of the needle (Fig. 3).

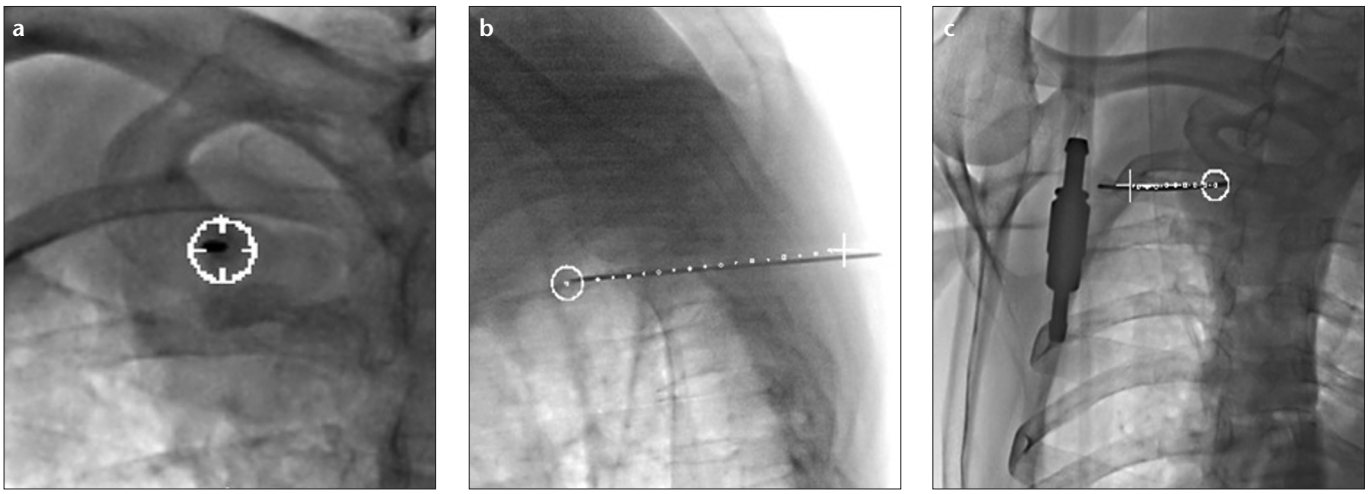

Figure 2. a–c. Real-time fluoroscopic images in "bull's eye view" **(a)** and two "progression views" **(b, c)**. The needle is advanced along the planned needle path *(dotted line)* from skin entry site *(white cross)* to target lesion site *(white circle)*.

PTNB technique

The patient was placed in either supine or prostrate position and administered local anesthesia. An automatic biopsy gun with 16-gauge needle, 15 cm needle length and 20 mm sample notch (Quick-Core; Cook Medical Inc., Bloomington, Indiana, USA) was used, and the needle was advanced along the planed path under real-time fluoroscopy. For sampling, the stylet was removed from the guiding needle and replaced by a biopsy needle, and approximately 1–2 cm of sample tissue was taken. This procedure could be repeated until sufficient tissue sample was obtained. The overall procedural time from the first 3D image acquisition for needle path planning to the removal of the needle with successfully obtained tissue sample was 14.6 ±1.5 minutes, resulting in a mean exposure dose of 224.4±74.8 mGy.

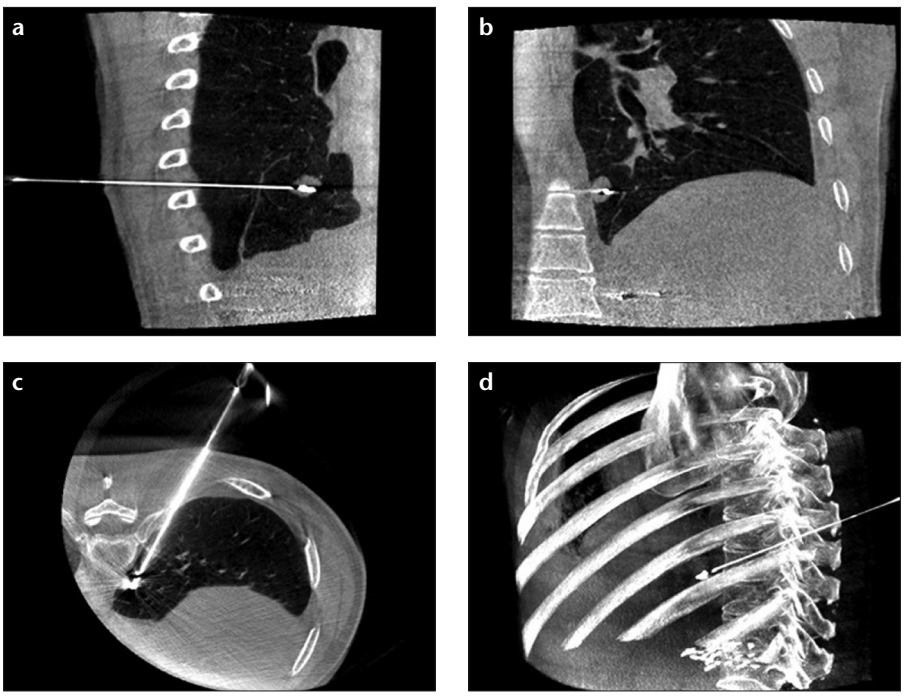

Figure 3. a–d. CBCT scan confirms the needle position in multiplanar **(a–c)** and volume rendering **(d)** images.

An erect chest radiograph was performed two hours after the procedure to detect any delayed complications such as hemorrhage or pneumothorax. Patients were observed in the hospital for 24 hours. In case of serious change in vital signs or clinical status, imaging was repeated and treatment was performed if necessary. The pulmonary lesions were considered to be benign if the histopathological results of biopsy demonstrated a specific and definitive benign histopathology such as granulomas, hamartomas, tuberculosis, or cryptococcosis; if the lesion's size was decreased 20% or more; and if the lesion did not show typical characteristics of malignant mass lesions during the two years of follow-up diagnostic imaging performed at four-month intervals.

Statistical analysis

McNemar test was used to compare two dependent categorical variables, namely PTNB results from CBCT-based 3D needle guidance system and final histopathological results.

Results

Histopathologic tissue was successfully obtained from 108 patients, yielding a puncture success rate of 98.2% (108/110). Access was achieved in all cases at the first needle pass. Two patients failed to complete PTNB procedure. One patient with chronic obstructive pulmonary disease and a 2 cm lesion developed severe pneumothorax with a volume of approximately 50% during the PTNB procedure. This patient then received a chest tube drainage therapy. The other patient had Alzheimer's disease and was unable to hold his breath properly, resulting in low image quality, which was

insufficient to perform the needle path planning. Therefore, the PTNB procedure was discontinued for this patient.

Among 108 successful PTNB cases, only one patient developed postoperative pneumothorax with volume over 30% and underwent chest tube drainage. There were 13 patients with pneumothorax volume within 10% and seven patients who developed self-limited mild hemoptysis for a maximum of 10 mL. These patients received no specific treatment as they were either asymptomatic or clinically stable, and the symptoms disappeared within three days. There was no associated air embolism, abscess, or hemothorax development in any of the patients. Detailed procedural and histopathological results were listed in Table 1. Among 108 pulmonary lesions, 91 lesions were malignant, and 17 lesions were benign. Three out of 91 malignant lesions were false negatives on PTNB, including biopsies of two patients that were interpreted as lung inflammation and one patient's biopsy that was interpreted as pulmonary tuberculosis. These three patients then received anti-inflammatory therapy. However, due to poor treatment outcomes, PTNB procedures were performed again in these patients and they were all confirmed with lung adenocarcinoma. As a result, PTNB of pulmonary lesions under CBCT-based 3D needle guidance was determined to have 97.2% (105/108) diagnostic accuracy, 96.7% (88/91) sensitivity, and 100% (17/17) specificity (Table 2). The final histopathological results and PTNB results from CBCT-based 3D needle guidance system were consistent ($P = 0.250$).

Table 1. Procedural results and histopathological outcomes of the patients who successfully underwent PTNB procedure with *syngo* iGuide needle guidance

	n (%)
Total no. of patients	110
Successful PTNB cases	108 (98.2)
Overall complications	21 (19.4)
Pneumothorax	14 (12.9)
Hemoptysis	7 (6.5)
Malignant histopathology (n=91)	
Lung adenocarcinoma	45 (49.4)
Squamous carcinoma	34 (37.4)
Small cell lung cancer	7 (7.7)
Mesothelioma of pleura	3 (3.3)
Carcinoid	1 (1.1)
Pulmonary blastoma	1 (1.1)
Benign histopathology (n=17)	
Lung inflammation	14 (82.4)
Pulmonary tuberculosis	3 (17.6)

Table 2. Diagnostic accuracy of the PTNB procedure according to lesion size

Lesion size	No. of patients	Correct diagnosis	Misdiagnosis	Accuracy (%)
≤2.0 cm	17	16	1	94.1
2–5 cm	71	70	1	98.6
≥5 cm	20	19	1	95.0

Discussion

In general, PTNB is a well-established, effective, and comparatively safe technique for the diagnosis of pulmonary lesions. This procedure is conventionally performed under CT- or CTF-guidance. However, these imaging techniques are often associated with limitations of in-plane imaging, real-time feedback, gantry sizes, etc. In our study, the PTNB procedures were all performed directly in the interventional radiology suite using a CBCT system with flexible system angulations capability, which offered superior access to obese patients, space for needles extending outside the body, and better image support for complex, double oblique needle trajectories. Moreover, the CBCT-based 3D needle guidance technique provided real-time fluoroscopic feedbacks and virtual navigation of biopsy needles, and thus, enabled optimal and safe needle path selections under convenient operating conditions.

Our results show that the CBCT-based 3D needle guidance technique, with its inherent advantages, effectively facilitates the needle progression procedure and provides accurate needle targeting of pulmonary lesions. This technique, based on the reconstructed CBCT images and real-time intraoperative navigation, provided a reliable tool to assist PTNB procedures even for very small lesions, and ensured a high puncture success rate of 98.2%. Diagnostic accuracy (97.2%) was found to be higher than those reported in previous studies of CT- or CTF-guided PTNB procedures (75%–90%). Besides, the procedural time could be kept within a limited range (12.5–17.5 minutes), which was much shorter than that of CT- or CTF-guided PTNB procedures (12.3–26.7 minutes). In addition, use of 3D needle guidance technique reduced the complication rates compared to the solely CBCT-guided PTNB procedures, although diagnostic results and procedural time were not significantly improved. In our study, the overall complication rate (19.4%), including pneumothorax rate (12.9%) and the hemoptysis rate (6.5%), was considerably lower, with only one patient requiring further intervention (0.9%). This low incidence of complications can be attributed to the use of CBCT-based 3D needle guidance technique, as the key advantage of this novel technique is acquisition of reconstructed 3D CBCT images immediately prior to

the PTNB procedure, clearly identifying internal organs, soft tissues, and bones. Therefore, an optimized access path for the needle insertion into the target pulmonary lesion can be determined based on the detailed anatomical information. In addition, based on the fluoroscopic feedbacks, this technique enables real-time monitoring of needle position and progression, such that any misalignment with the planned path can be corrected immediately, and the actual needle trajectory can be adjusted to minimize complications correlated with respiration movement. Precise localization and documentation of the biopsy needle and target lesion allow clinicians to perform PTNB procedures with increased confidence within a shorter timeframe, resulting in an enhanced clinical workflow and less radiation exposure-induced adverse health effects.

The limitations of this technique should also be mentioned. As patient movements may result in motion artifacts and affect the registration accuracy of the projected path, the key factor for achieving successful needle guidance is to generate high-quality 3D CBCT images. To this aim, during the imaging procedure, the patient should be well-stabilized. However, this requirement may not be fulfilled and limits its application for some patients who have difficulty sustaining a breathhold for the duration of imaging.

In conclusion, this preliminary study shows that the CBCT-based 3D needle guidance technique enables reliable and accurate needle positioning and progression by providing real-time intraoperative guidance. This new technique has great potential for applications in PTNB procedures for pulmonary lesions, resulting in high diagnostic accuracy and low complication rates. Furthermore, the above described technique may also be applied in different puncture procedures.

Conflict of interest disclosure

The authors declared no conflicts of interest.

References

1. Munden RF, Pugatch RD, Liptay MJ, Sugarbaker DJ, Le LU. Small pulmonary lesions detected at CT: clinical importance. Radiology 1997; 202:105–110. [CrossRef]
2. Berger WG, Erly WK, Krupinski EA, Standen JR, Stern RG. The solitary pulmonary nodule on chest radiography: can we really tell if the nodule is calcified? AJR Am J Roentgenol 2001; 176:201–204. [CrossRef]
3. Choi JW, Park CM, Goo JM, et al. C-arm cone-beam CT-guided percutaneous transthoracic needle biopsy of small (≤ 20 mm) lung nodules: diagnostic accuracy and complications in 161 patients. AJR Am J Roentgenol 2012; 199:W322–330. [CrossRef]
4. Cheung JY, Kim Y, Shim SS, Lim SM. Combined fluoroscopy- and CT-guided transthoracic needle biopsy using a C-arm cone-beam CT system: comparison with fluoroscopy-guided biopsy. Korean J Radiol 2011; 12:89–96. [CrossRef]
5. Hiraki T, Mimura H, Gobara H, et al. CT fluoroscopy guided biopsy of 1000 pulmonary lesions performed with 20-gauge coaxial cutting needles: diagnostic yield and risk factors for diagnostic failure. Chest 2009; 136:1612–1617. [CrossRef]
6. Kim GR, Hur J, Lee SM, et al. CT fluoroscopy-guided lung biopsy versus conventional CT-guided lung biopsy: a prospective controlled study to assess radiation doses and diagnostic performance. Eur Radiol 2011; 21:232–239. [CrossRef]
7. Braak SJ, van Strijen MJ, van Leersum M, van Es HW, van Heesewijk JP. Real-time 3D fluoroscopy guidance during needle interventions: technique, accuracy, and feasibility. AJR Am J Roentgenol 2010; 194:W445–W451. [CrossRef]
8. Priola AM, Priola SM, Cataldi A, et al. Accuracy of CT guided transthoracic needle biopsy of lung lesions: factors affecting diagnostic yield. Radiol Med 2007; 112:1142–1159. [CrossRef]
9. vanSonnenberg E, Casola G, Ho M, et al. Difficult thoracic lesions: CT-guided biopsy experience in 150 cases. Radiology 1988; 167:457–461. [CrossRef]
10. Kurban LA, Gomersall L, Weir J, Wade P. Fluoroscopy-guided percutaneous lung biopsy: a valuable alternative to computed tomography. Acta Radiol 2008; 49:876–882. [CrossRef]
11. Laurent F, Latrabe V, Vergier B, Montaudon M, Vernejoux JM, Dubrez J. CT-guided transthoracic needle biopsy of pulmonary nodules smaller than 20 mm: results with an automated 20-gauge coaxial cutting needle. Clin Radiol 2000; 55:281–287. [CrossRef]
12. Muehlstaedt M, Bruening R, Diebold J, Mueller A, Helmberger T, Reiser M. CT/fluoroscopy-guided transthoracic needle biopsy: sensitivity and complication rate in 98 procedures. J Comput Assist Tomogr 2002; 26:191–196. [CrossRef]
13. Wallace MJ, Krishnamurthy S, Broemeling LD, et al. CT-guided percutaneous fine-needle aspiration biopsy of small (< or =1-cm) pulmonary lesions. Radiology 2002; 225:823–828. [CrossRef]
14. Heck SL, Blom P, Berstad A. Accuracy and complications in computed tomography fluoroscopy-guided needle biopsies of lung masses. Eur Radiol 2006; 16:1387–1392. [CrossRef]
15. Akpek S, Brunner T, Benndorf G, Strother C. Three-dimensional imaging and cone beam volume CT in C-arm angiography with flat panel detector. Diagn Interv Radiol 2005; 11:10–13.
16. Kalender WA, Kyriakou Y. Flat-detector computed tomography (FD-CT). Eur Radiol 2007; 17:2767–2779. [CrossRef]
17. Fahrig R, Fox AJ, Lownie S, Holdsworth DW. Use of a C-arm system to generate true 3-D computed rotational angiograms: Preliminary in vitro and in vivo results. AJNR Am J Neuroradiol 1997; l8:1507–1514.
18. Jin KN, Park CM, Goo JM, et al. Initial experience of percutaneous transthoracic needle biopsy of lung nodules using C-arm cone-beam CT systems. Eur Radiol 2010; 20:2108–2115. [CrossRef]
19. Hwang HS, Chung MJ, Lee JW, Shin SW, Lee KS. C-arm cone-beam CT-guided percutaneous transthoracic lung biopsy: usefulness in evaluation of small pulmonary nodules. AJR Am J Roentgenol 2010; 195:W400–407. [CrossRef]
20. Lee SM, Park CM, Lee KM, Bahn YE, Kim JI, Goo JM. C-arm cone-beam CT-guided percutaneous transthoracic needle biopsy of lung nodules: clinical experience in 1108 patients. Radiology 2014; 271:291–300. [CrossRef]
21. Choo JY, Park CM, Lee NK, et al. Percutaneous transthoracic needle biopsy of small (</=1 cm) lung nodules under C-arm cone-beam CT virtual navigation guidance. Eur Radiol 2013; 23:712–719. [CrossRef]
22. Choi MJ, Kim Y, Hong YS, Shim SS, Lim SM, Lee JK. Transthoracic needle biopsy using a C-arm cone-beam CT system: diagnostic accuracy and safety. Br J Radiol 2012; 85:e182–187. [CrossRef]
23. Lee WJ, Chong S, Seo JS, Shim HJ. Transthoracic fine-needle aspiration biopsy of the lungs using a C-arm cone-beam CT system: diagnostic accuracy and post-procedural complications. Br J Radiol 2012; 85:e217–222. [CrossRef]
24. Busser WM, Braak SJ, Fütterer JJ, et al. Cone beam CT guidance provides superior accuracy for complex needle paths compared with CT guidance. Br J Radiol 2013; 86:20130310. [CrossRef]
25. Morimoto M, Numata K, Kondo M, et al. C-arm cone beam CT for hepatic tumor ablation under real-time 3D imaging. AJR Am J Roentgenol 2010; 194:W452–W454. [CrossRef]